

RKCL4232

**LIMITING HIGH PRESSURE RATE COEFFICIENTS FOR THE
HO+NO₂→HONO₂ REACTION ON *AB INITIO* POTENTIAL ENERGY
SURFACES**

Carlos J. Cobos

Instituto de Investigaciones Físicoquímicas Teóricas y Aplicadas (INIFTA), Departamento de
Química, Facultad de Ciencias Exactas, Universidad Nacional de La Plata, CONICET, CICBA,
Casilla de Correo 16, Sucursal 4, (1900) La Plata, Argentina

Received October 28, 2002

Accepted January 13, 2003

Abstract

Phase space limiting high pressure rate coefficients for the title reaction on *ab initio* potential energy surfaces have been calculated at 50-600 K. Calculated rigidity factors at different levels of theory are presented. The best limiting high pressure rate coefficient obtained at 300 K, $4.0 \times 10^{-11} \text{ cm}^3 \text{ molecule}^{-1} \text{ s}^{-1}$, compares very well with the latest IUPAC recommended value.

Keywords: Limiting high pressure rate coefficient, potential energy surface, HONO₂

INTRODUCTION

The recombination reaction of HO radical with NO₂ to form HONO₂ is a key process in both tropospheric and stratospheric chemistry. By removing HO and NO₂ into stable HONO₂, partially responsible for acid precipitation, this process couples the odd-hydrogen and odd-nitrogen families and terminates important catalytic cycles involving these radicals [1]. Due to the fact that global atmospheric models are particularly sensitive to the rate coefficient of this reaction, it has been extensively studied [2-5]. Despite of this, discrepancies remain, mainly at the higher part of the falloff curve that describes the pressure dependence of the rate coefficients. In particular, the limiting high pressure rate coefficients k_{∞} recommended for a long time at the

NASA compilation [2] is more than a factor of four smaller than that given by the IUPAC [3]. This fact is consistent with experimental values ranging from 1.5×10^{-11} [6] to 7.5×10^{-11} $\text{cm}^3 \text{ molecule}^{-1} \text{ s}^{-1}$ [7] at 300 K. At present the difference is smaller, the latest recommended values $(1.8 \pm 0.2) \times 10^{-11}$ $\text{cm}^3 \text{ molecule}^{-1} \text{ s}^{-1}$ [4] being and $(4.1 \pm 2) \times 10^{-11}$ $\text{cm}^3 \text{ molecule}^{-1} \text{ s}^{-1}$ [5]. The discrepancies mentioned have been partly attributed to differences in the falloff extrapolation procedures employed and most probably to formation of the stable HOONO isomer through an alternative reactive channel.

This Letter is concerned with a theoretical study of the title reaction employing two versions of the statistical adiabatic channel model (SACM) [8-11] coupled with potential energy surfaces based on density functional theory (DFT) and *ab initio* molecular orbital calculations.

THEORETICAL FORMALISM, RESULTS AND DISCUSSION

In the frame of the SACM [8] the limiting high pressure rate coefficient for a recombination reaction is given by $k_{\infty} = f_{\text{rigid}} k_{\infty}(\text{PST})$ [9]. Here $k_{\infty}(\text{PST})$ is limiting high pressure rate coefficient provided by the phase space theory and f_{rigid} is the so-called rigidity factor. $k_{\infty}(\text{PST})$ is exclusively determined by the interplay between the isotropic part of the electronic potential and the centrifugal potential, and provides an upper bound to the rate coefficients. On the other hand, $f_{\text{rigid}} \leq 1$ accounts for the contraction of the available phase space due to the anisotropy of the transitional motions. $k_{\infty}(\text{PST})$ is calculated as

$$k_{\infty}(\text{PST}) = (kT/h)(h^2/2\pi\mu kT)^{3/2} [1/(2(2+2\exp(-201/T)))] \sum_{J=0}^{\infty} (2J+1) \exp\{-[E_0(J)-E_0(J=0)]/kT\} \quad (1)$$

where k is Boltzmann's constant, h is Planck's constant, T is the absolute temperature, μ is the collisional reduced mass, while the third factor, in brackets, accounts for electronic degeneracy and the sum takes into account relevant centrifugal effects. $E_0(J)$ denotes centrifugal energy barriers as a function of the total angular momentum J , obtained from the maxima of the channel potential $V_{\text{cent}}(J,r) = V(r) + B_{\text{eff}}(r)J(J+1)$. Here $V(r)$ is the electronic potential along the reaction coordinate r (the HO-NO₂ bond distance) and $B_{\text{eff}}(r) = [A(r) + B(r)]/2$ the effective rotational constant. Calculations similar to the present can be found elsewhere [8,9,11-15].

Different quantum chemical approaches were employed to estimate $V(r)$, while $B_{\text{eff}}(r)$ values were derived from fully optimized geometries obtained with the B3LYP hybrid functional [16,17] in conjunction with the large 6-311++G(3df,3pd) basis set. *Ab initio* single point energy calculations on DFT

structures were employed to compute the electronic potential. In this way, in addition to the UB3LYP/6-311++G(3df,3pd) potential (potential I), values for $V(r)$ at the PMP2/6-311++G(2df,2pd)//UB3LYP/6-311++G(3df,3pd) (potential II) level were calculated. Our best estimations were performed at the high correlated coupled cluster singles and doubles approach, including a perturbational estimate of the triple excitations [18]: UCCSD(T)/6-311++G(2df,2pd)//UB3LYP/6-311++G(3df,3pd) (potential III) and UCCSD(T)/cc-pVTZ//UB3LYP/6-311++G(3df,3pd) (potential IV). The 6-311++G(2df,2pd) basis is formed by a total number of 151 basis functions while the cc-pVTZ basis contains 134. Coupled cluster methods are relatively insensitive to spin contamination and to the multireference character of the wavefunctions. In addition, alfa-beta and spatial spin symmetries were destroyed by mixing HOMO and LUMO to obtain accurate unrestricted wavefunctions for singlet states. The Gaussian 98 program [19] was used in all calculations.

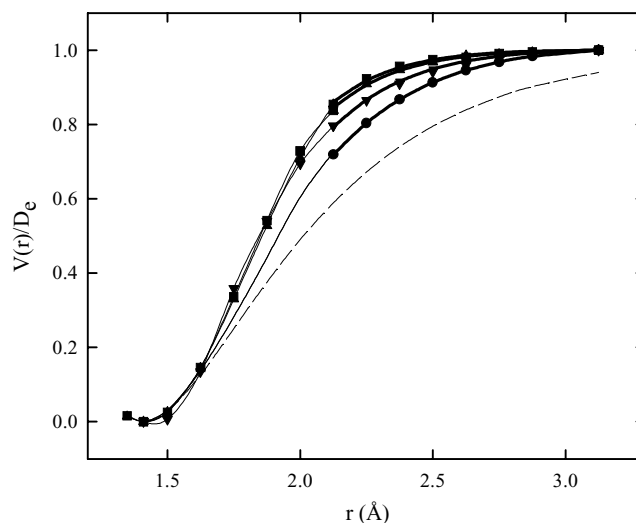


Fig. 1. Dependence of the normalized electronic potentials on the HO-NO₂ bond distance. ●: UB3LYP/6-311++G(3df,3pd); ▼: PMP2/6-311++G(2df,2pd)//UB3LYP/6-311++G(3df,3pd); ▲: UCCSD(T)/6-311++G(2df,2pd)//UB3LYP/6-311++G(3df,3pd); ■: UCCSD(T)/cc-pVTZ//UB3LYP/6-311++G(3df,3pd). ---: Morse potential with $\beta_{eq}=2.04 \text{ \AA}^{-1}$. The solid lines above $r=2.1 \text{ \AA}$ are the results of the fits described in the text

To compare the shapes of the potential energy curves, reduced $V(r)/D_e$ values are depicted in Fig. 1. Parts of the potentials relevant in the kinetic calculations (located above 2.1 Å) were fitted with a Varshni potential function $V(r)/D_e = \{1 - (r_e/r) \exp[-\gamma(r^2 - r_e^2)]\}^2$ (with $r_e = 1.410$ Å) [20]. γ and D_e values for each potential are: $\gamma = 0.5706$ Å⁻² and $D_e = 49.3$ kcal mol⁻¹ (potential I), $\gamma = 0.7079$ Å⁻² and $D_e = 52.4$ kcal mol⁻¹ (potential II), $\gamma = 0.8308$ Å⁻² and $D_e = 50.7$ kcal mol⁻¹ (potential III) and $\gamma = 0.8754$ Å⁻² and $D_e = 50.8$ kcal mol⁻¹ (potential IV). A standard Morse potential $V(r)/D_e = \{1 - \exp[-\beta(r - r_e)]\}^2$ calculated with $\beta = 2.04$ Å⁻¹ [11] is shown in Fig. 1 for comparison. The calculated Morse attractive interaction between HO and NO₂ is much larger than that predicted employing the quantum chemical potentials. However, as before, the higher part of the UCCSD(T)/6-311++G(2df,2pd)//UB3LYP/6-311++G(3df,3pd) potential can be very well represented by using $\beta = 4.18$ Å⁻¹ (Potential V). As Fig. 1 shows, the rest of the calculated potential curves lie between those calculated with the standard Morse and with the coupled cluster method.

Effective rotational constants estimated at the UB3LYP/6-311++G(3df,3pd) level from HO-NO₂ values ranging from 1.410 to 3.125 Å were accurately fitted with the function $B_{\text{eff}}(r) = 0.3071 / (1 + 0.6670(r - r_e) + 0.3090(r - r_e)^2)$. $k_{\infty}(\text{PST})$ values calculated with equation (1) and potentials I to V are listed in Table 1.

Table 1

Calculated $k_{\infty}(\text{PST})$ values (in units of cm³ molecule⁻¹ s⁻¹) for reaction HO+NO₂→HONO₂ at different quantum chemical levels

T(K)	Potential I	Potential II	Potential III	Potential IV	Potential V
50	5.16x10 ⁻¹¹	4.38x10 ⁻¹¹	3.90x10 ⁻¹¹	3.76x10 ⁻¹¹	4.15x10 ⁻¹¹
100	6.09x10 ⁻¹¹	5.20x10 ⁻¹¹	4.64x10 ⁻¹¹	4.48x10 ⁻¹¹	4.54x10 ⁻¹¹
200	6.62x10 ⁻¹¹	5.67x10 ⁻¹¹	5.09x10 ⁻¹¹	4.92x10 ⁻¹¹	5.15x10 ⁻¹¹
300	6.97x10 ⁻¹¹	6.00x10 ⁻¹¹	5.40x10 ⁻¹¹	5.22x10 ⁻¹¹	5.39x10 ⁻¹¹
400	7.32x10 ⁻¹¹	6.31x10 ⁻¹¹	5.69x10 ⁻¹¹	5.51x10 ⁻¹¹	5.63x10 ⁻¹¹
500	7.64x10 ⁻¹¹	6.31x10 ⁻¹¹	5.97x10 ⁻¹¹	5.78x10 ⁻¹¹	5.86x10 ⁻¹¹
600	7.95x10 ⁻¹¹	6.89x10 ⁻¹¹	6.25x10 ⁻¹¹	6.04x10 ⁻¹¹	6.09x10 ⁻¹¹

All calculated rate coefficients exhibit a small positive temperature dependence. On the other hand, only small basis set effects on $k_{\infty}(\text{PST})$ are observed from calculations performed with potentials III and IV. The present accurate upper limit for the rate coefficient computed at 300 K of

$5.3 \times 10^{-11} \text{ cm}^3 \text{ molecule}^{-1} \text{ s}^{-1}$ lies between the above mentioned recommended NASA [2] and IUPAC [3] k_{∞} values. This suggests that the latter ones appear to be too high, probably due to the concurrence of channels forming HONO₂ and HOONO. The more recent recommendation available from the IUPAC website [5] gives a value of $(4.1 \pm 2) \times 10^{-11} \text{ cm}^3 \text{ molecule}^{-1} \text{ s}^{-1}$ at 200-400 K which is lower than the former recommendation but yet higher than that suggested by NASA, $(1.8 \pm 0.2) \times 10^{-11} \text{ cm}^3 \text{ molecule}^{-1} \text{ s}^{-1}$ [4].

Combining the values of refs [4] and [5] with our best room temperature k_{∞} (PST), “experimental” rigidity factors of 0.3 and 0.8 result. Due to the fact that f_{rigid} typically ranges from about 0.002 to 0.6 [9,13], the present value seems to be the highest reported so far. It should be noted that an accurate “a priori” estimation of f_{rigid} is a difficult task which requires a correct characterization of the transitional modes along the minimum energy path, only available by high-level *ab initio* methods. The first SACM approach for f_{rigid} is based on a standard Morse function to represent the radial potential and an exponential decay of the transitional modes, namely $\omega \approx \omega_e \exp[-\alpha(r-r_e)]$, to model the angular potentials [9]. An anisotropic parameter of $\alpha/\beta \approx 0.5$ reproduces satisfactorily the experimental k_{∞} values of a large number of recombination reactions [9]. However, for the present system, large α/β values of 0.73 and 0.79 are required to reproduce the average consensus value of $k_{\infty} = 3 \times 10^{-11} \text{ cm}^3 \text{ molecule}^{-1} \text{ s}^{-1}$ ($f_{\text{rigid}} = 0.56$) with either the standard Morse ($\beta = 2.04 \text{ \AA}^{-1}$) or with the potential V ($\beta = 4.18 \text{ \AA}^{-1}$). The very small $f_{\text{rigid}} = 0.008$ obtained with $\beta = 4.18 \text{ \AA}^{-1}$ and a normal $\alpha/\beta = 0.5$ indicates that this reaction behaves anomalously. To our knowledge, no other reactions studied exhibit so large α/β values.

An improved version named SACM/CT [10] that couples SACM with classical trajectory calculations on valence potentials has been recently developed to study capture rate coefficients between two linear rotors forming either linear or nonlinear complexes. Assuming an energized HONO₂ adduct with a perpendicular arrangement of HO and NO₂ rotors, Troe [11] estimates rigidity factors (for $\alpha/\beta = 0.5$) of 0.82 at 0 K and of about 0.66 at 300 K. We have employed the SACM/CT approach using the same molecular input data of ref [11] to calculate $k_{\infty} = f_{\text{rigid}} k_{\infty}$ (PST) with our coupled cluster/Morse potential (Potential V). Under this conditions, the $f_{\text{rigid}}(T \rightarrow 0) = 0.82$ value of ref. [11] is reduced, over the temperature range 200-400 K, to about 0.75. These results indicate that the current reaction is close to its phase space limit and, therefore, the importance of an accurate knowledge of k_{∞} (PST) is evident. In addition, the model predicts $f_{\text{rigid}}(T \rightarrow 0)$ values of 0.084 and 0.98 for α/β parameters of 0.3 and 0.7. The resulting k_{∞} , which is almost independent of temperature under typical atmospheric conditions, is

$$k_{\infty} = 4.0 \times 10^{-11} \text{ cm}^3 \text{ molecule}^{-1} \text{ s}^{-1}$$

The estimated value agrees very well with that obtained by Troe [11] from extrapolation of the falloff curves of ref. [21] of $3.6 \times 10^{-11} \text{ cm}^3 \text{ molecule}^{-1} \text{ s}^{-1}$, and with that recommended by the latest IUPAC compilation of $(4.1 \pm 2) \times 10^{-11} \text{ cm}^3 \text{ molecule}^{-1} \text{ s}^{-1}$ [5]. On the other hand, recent laser flash photolysis/LIF experiments by Hippler and co-workers [22] provide convincing evidence for HOONO isomer formation. They were able to separate temporally $\text{HO} + \text{NO}_2 + \text{He} \rightarrow \text{HONO}_2 + \text{He}$ and $\text{HO} + \text{NO}_2 + \text{He} \rightarrow \text{HOONO} + \text{He}$ reactions, and measure the respective absolute rate coefficients from 5 to 94 atm. It is interesting to note that the highest value they measure at 430 K, $2.1 \times 10^{-11} \text{ cm}^3 \text{ molecule}^{-1} \text{ s}^{-1}$, does not appear to have yet reached the high pressure regime. Finally, if the formation of HONO_2 and HOONO are truly separated processes and the experiments of ref. [7] ($k_{\infty} = 7.5 \times 10^{-11} \text{ cm}^3 \text{ molecule}^{-1} \text{ s}^{-1}$) yield a measure of the sum of the rate coefficients, the present results indicate that similar k_{∞} should be expected for both channels.

In summary, the present high-level *ab initio* potential data implemented in SACM/CT calculations leads to limiting high pressure rate coefficients for the title reaction which are in very good agreement with latest IUPAC recommended value [5]. Further quantum chemical studies are being undertaken to characterize the anisotropic potential in order to improve f_{rigid} .

Acknowledgements. This work was supported by the Universidad Nacional de La Plata, the Consejo Nacional de Investigaciones Científicas y Técnicas (CONICET, PIP 0450), the Comisión de Investigaciones Científicas de la Provincia de Buenos Aires (CICBA) and the Agencia Nacional de Promoción Científica y Tecnológica (PICT 6786). The author is grateful to Prof. Jürgen Troe for helpful discussions.

REFERENCES

1. H. Johnston: *Science*, **173**, 517 (1971).
2. W.B. DeMore, S.P. Sander, D.M. Golden, R.F. Hampson, M.J. Kurylo, C.J. Howard, A.R. Ravishankara, C.E. Kolb, M.J. Molina: *Chemical Kinetics and Photochemical Data for Use in Stratospheric Modeling*. Evaluation 12, NASA/JPL, Publication 97-4, Pasadena, CA, 1997.
3. R. Atkinson, D.L. Baulch, R.A. Cox, R.F. Hampson, J.A. Kerr, M.J. Rossi, J. Troe: *J. Phys. Chem. Ref. Data*, **26**, 1329 (1997) and references therein.
4. S.P. Sander, R.R. Friedl, W.B. DeMore, D.M. Golden, M.J. Kurylo, R.F. Hampson, R.E. Huie, G.K. Moortgat, A.R. Ravishankara, C. E. Kolb, M. J. Molina: *Chemical Kinetics and Photochemical Data for Use in Stratospheric Modeling*. NASA/JPL, Publication 00-3, Pasadena, CA, 2000. <http://jpldataeval.jpl.nasa.gov/>.

5. IUPAC Subcommittee for Gas Kinetic Data Evaluation. Web Version December 2001, by R.G. Hynes, G.D. Garver, R.A. Cox: <http://www.iupac-kinetic.ch.cam.ac.uk/> and references therein.
6. S.S. Brown, R.A. Talukdar, A.R. Ravishankara: *Chem. Phys. Lett.*, **299**, 277 (1999).
7. D. Fulle, H.F. Hamann, H. Hippler, J. Troe: *J. Chem. Phys.*, **108**, 5391 (1998).
8. J. Troe: *J. Chem. Phys.*, **75**, 226 (1981).
9. C.J. Cobos, J. Troe: *J. Chem. Phys.*, **83**, 1010 (1985).
10. A.I. Maergoiz, E.E. Nikitin, J. Troe, V.G. Ushakov: *J. Chem. Phys.*, **108**, 5265 (1998).
11. J. Troe: *Int. J. Chem. Kinet.*, **33**, 878 (2001).
12. C.J. Cobos: *J. Chem. Phys.*, **85**, 5644 (1986).
13. C.J. Cobos: *React. Kinet. Catal. Lett.*, **49**, 167 (1993).
14. A.E. Croce, C.J. Cobos, E. Castellano: *Chem. Phys.*, **211**, 215 (1996).
15. C.J. Cobos: *React. Kinet. Catal. Lett.*, **69**, 379 (2000).
16. A.D. Becke: *Phys. Rev. A*, **38**, 3098 (1988).
17. C. Lee, W. Yang, R.G. Parr: *Phys. Rev. B*, **37**, 785 (1988).
18. J.A. Pople, M. Head-Gordon, K. Raghavachari: *J. Chem. Phys.*, **87**, 5968 (1987).
19. M.J. Frisch, G.W. Trucks, H.B. Schlegel, G.E. Scuseria, M.A. Robb, J.R. Cheeseman, V.G. Zakrzewski, J.A. Montgomery, Jr., R.E. Stratmann, J.C. Burant, S. Dapprich, J.M. Millam, A.D. Daniels, K.N. Kudin, M.C. Strain, O. Farkas, J. Tomasi, V. Barone, M. Cossi, R. Cammi, B. Mennucci, C. Pomelli, C. Adamo, S. Clifford, J. Ochterski, G.A. Petersson, P.Y. Ayala, Q. Cui, K. Morokuma, D.K. Malick, A.D. Rabuck, K. Raghavachari, J.B. Foresman, J. Cioslowski, J.V. Ortiz, A.G. Baboul, B.B. Stefanov, G. Liu, A. Liashenko, P. Piskorz, I. Komaromi, R. Gomperts, R.L. Martin, D.J. Fox, T. Keith, M.A. Al-Laham, C.Y. Peng, A. Nanayakkara, C. Gonzalez, M. Challacombe, P.M.W. Gill, B. Johnson, W. Chen, M.W. Wong, J.L. Andres, C. Gonzalez, M. Head-Gordon, E.S. Replogle, J.A. Pople: *Gaussian 98*, Revision A.7, Gaussian, Inc., Pittsburgh PA, 1998.
20. Y.P. Varshni: *Rev. Mod. Phys.* **29**, 664 (1957).
21. T.J. Dransfield, K.K. Perkins, N.M. Donahue, J.G. Anderson, M.M. Sprenguerther, K.L. Demerjian: *Geophys. Res. Lett.*, **26**, 687 (1999).
22. H. Hippler, S. Nasterlack, F. Striebel: *Phys. Chem. Chem. Phys.*, **4**, 2959 (2002).